PRE-TENSIONED STEEL CABLES EXPOSED TO LOCALISED FIRES

Yong Du[1,2,3], J.Y. Richard Liew[1,3], Hao Zhang[1] and Guoqiang-Li[2]

[1]*Nanjing Tech University, College of Civil Engineering, Jiangsu, 211800, China*
[2]*Civil Engineering Disaster Prevention National Key Laboratory, Shanghai, 200092, China*
[3]*National University of Singapore, Department of Civil & Environmental Engineering, 117576, Singapore*
**(Corresponding author: E-mail: yongdu_mail@njtech.edu.cn)*

Received: 30 November 2016; Revised: 23 May 2017; Accepted: 13 June 2017

ABSTRACT: Pre-tensioned steel cables are often used in hybrid string structures, suspended roofs and cable suspended bridges. When subjected to localised fire, the tensile force in the steel cables reduces due to thermal expansion, and thus, the geometry of the structure and the internal force distribution in the cable-tensioned structure will be affected. The mechanical behavior of pre-tensioned steel cables is sensitive to the elevated temperature history. In this paper, a set of analytical formulation has been proposed to determine the transient tension force in a cable subjected to localised heating considering the mechanical properties at elevated temperature and the effects of loading configuration, pre-tensioned force level, and thermal expansion at elevated temperature. The fire resistance of a pre-tensioned steel cable can be determined when the cable tension force is equal to its effective yield strength at elevated temperature. Meanwhile, the proposed method is able to capture the relationship between the transient tension forces with each influence parameter in order to study the behavior of steel cables subjected to localised fire. The mechanical responses predicted by the proposed analytical method of pre-tensioned cables exposed to localised fires are validated against the numerical results obtained from nonlinear finite element software. Finally, a design flow chart is proposed for fire resistant design of pre-tensioned steel cables and the calculations can be implemented using a spreadsheet program.

Keywords: Cable-tensioned structure, fire resistance, localised fire, pre-tensioned structure, steel cable

DOI: 10.18057/IJASC.2018.14.2.5

1. INTRODUCTION

Pre-tensioned structures, such as beam string structures and suspension domes, are applicable for large space buildings or long span bridges. Typical pre-tensioned members are steel cables, steel rods or chains and they are generally named as ‘string’ in hybrid string structures. The steel cable is the most commonly used as a pre-tensioned member in hybrid string structures because of its high strength and the ease of applying tension force [1]. Fire induced high temperature can cause damage to pre-tensioned structures. For example, an aircraft warehouse with pre-tensioned truss in Brussels International airport collapsed in fire, shown in Figure 1, just as the roof of Ji’nan Olympic Stadium in China with cable suspension dome damaged in fire, as shown in Figure 2.

There is an abundance of research on behaviour of tensioned structures at ambient temperature [1]~[3]. As shown in Figure 3 and 4, a large number of cases has been located in China. Zhou [4] studied the fire resistance of cable suspended structures exposed to standard ISO fire, and determined that a cable suspended structure under ISO fire hold similar displacement as a pre-tensioned cable. Sheng [5] and Fan [6] studied the mechanical behaviours of beam string structures and suspension domes exposed to localised fire respectively. In the work by Wang et al. [7] and the manual for post-tensioned concrete[8], the Young’s Modulus and yield strength of steel wires at elevated temperature have been reported based on experimental investigation. It should be noted that analysis of fire resistance of tension structures is mainly done by numerical method, and there are limited data for pre-tensioned steel cable or tensioned structure tested at elevated

temperature. Although the final aim of the study is to determine the fire resistance capability of tension structures, the first step is to determine the mechanical response of pre-tensioned cables exposed to localised fire. The fire resistance of a pre-tensioned cable can be established by comparing the transient horizontal tension force in cables throughout the whole fire history with the effective yield strength of the cable. The analytical method proposed in this paper would be useful for analysing the structural response of cable suspended buildings, beam string structures or suspension bridges exposed to localized fires.

Figure 1. Collapse of the Aircraft Warehouse of Brussels International Airport after Fire

Figure 2. Ji'nan Olympic Stadium in China Damaged in Fire

Figure 3. Pudong International Airport in Shanghai, China

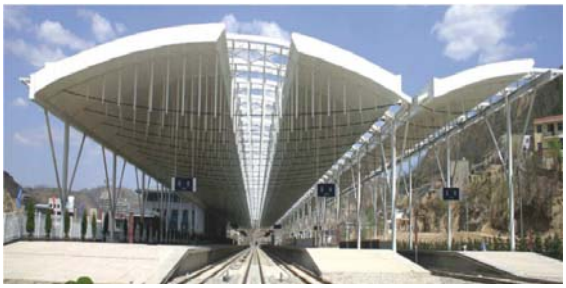

Figure 4. Train Station Platform, in Yan-an City, China

There is an abundance of research on behaviour of tensioned structures at ambient temperature [1]~[3]. As shown in Figure 3 and 4, a large number of cases has been located in China. Zhou [4] studied the fire resistance of cable suspended structures exposed to standard ISO fire, and determined that a cable suspended structure under ISO fire hold similar displacement as a pre-tensioned cable. Sheng [5] and Fan [6] studied the mechanical behaviours of beam string structures and suspension domes exposed to localised fire respectively. In the work by Wang et al. [7] and the manual for post-tensioned concrete [8], the Young's Modulus and yield strength of steel wires at elevated temperature have been reported based on experimental investigation. It should be noted that analysis of fire resistance of tension structures is mainly done by numerical method, and there are limited data for pre-tensioned steel cable or tensioned structure tested at elevated temperature. Although the final aim of the study is to determine the fire resistance capability of tension structures, the first step is to determine the mechanical response of pre-tensioned cables exposed to localised fire. The fire resistance of a pre-tensioned cable can be established by comparing the transient horizontal tension force in cables throughout the whole fire history with the effective yield strength of the cable. The analytical method proposed in this paper would be useful for analysing the structural response of cable suspended buildings, beam string structures or suspension bridges exposed to localized fires.

2. MODELLING OF PRE-TENSIONED CABLES IN FIRES

2.1 Modelling of Localised Fires

Figure 5 shows a steel cable, simply supported at both ends, is exposed to a localized fire. The temperature distribution in the cable is non-uniform in nature with hot smoke tends to accumulate at the ceiling level and the temperature distribution varies in accordance with the flame radiation which is related to the distance of the cable with respect to the fire source, as shown in Figure 5. From the vertical axis of plume centre, the temperature reduces symmetrically following the distance '*x*' from the fire source, as shown in Figure 6, which is generated from a CFD fire simulation[13].

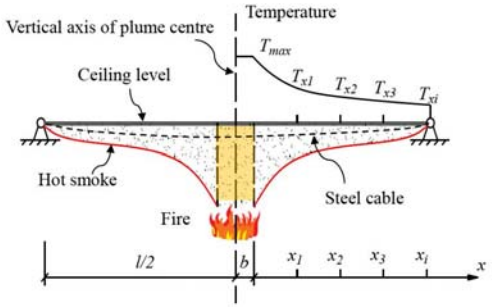

Figure 5. Effects of Hot Smoke and Flame on the Steel Cable

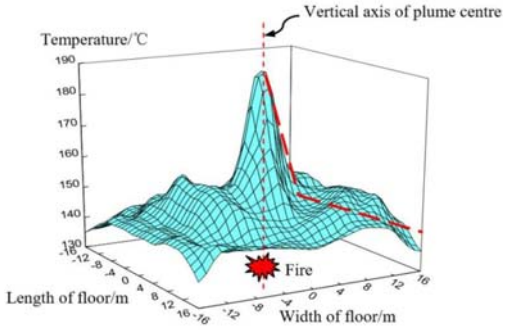

Figure 6. Typical Transient Temperature Distribution in Localized Fire

There are many models to predict the temperature distribution in localised fires, e.g. localised fires in EN 1991-1-2 [9], ASTM Standard E119-05 [10] and large space fires in NFPA 92B [11]. CECS200:2006[12] and Du et al.[13] describe the temperature distribution based on the field model given as:

$$T = T_{\max} f(x) = T_{\max}\left[\eta + (1-\eta)\exp\left(\frac{b-x}{7}\right)\right] \quad (1)$$

where b is the effective radius of fire source, taken as $b = \sqrt{A_q/\pi}$; A_q is the area of the fire source; $T_{\max}$ is the maximum temperature above the fire source, as shown in Figure 7; x is the distance from the vertical axis of plume centerline as shown in Figure 6; $f(x)$ is the regressing function of temperature shown in Figure 7 with a range of factor η which is the reduction factor of temperature depending on the floor area, Asp, and ceiling height, *H*, given in Table 1 [13].

There are three cases that the area of the fire source cannot be ignored. One is short spanning cable in which the size of the fire source "*b*" is relatively important as it affects the temperature distribution in the cable. The second is the area of the fire source becomes much larger from 9m^2 up to 50m^2. The third is the cable is far away from the fire source. If the area of the fire source cannot

be ignored, the length of the cable right above the fire source of size "*b*" will be subjected to the maximum temperature during the fire history. In most cases, the length of the cable is much longer than the size of the fire resource as the cables are usually employed by long span buildings.

Table 1. Reduction Factor η with Volumes of Large Space Buildings

A_{sp} (m^2)	H (m)				
	6	9	12	15	20
500	0.60	0.65	0.70	0.80	0.85
1000	0.50	0.55	0.60	0.70	0.75
3000	0.40	0.45	0.50	0.55	0.60
6000	0.25	0.30	0.40	0.45	0.50

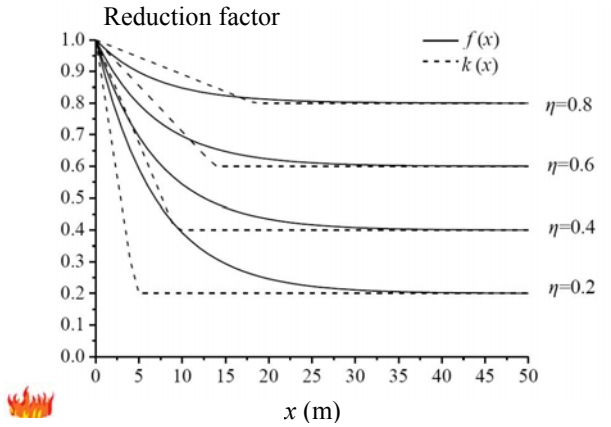

Figure 7. Regression Function Versus the Distance from the Vertical Axis of Plume Centerline with Varying η

Function $f(x)$ is a complex equation in which integration cannot be performed. *A* simplified bi-linear model $k(x)$ is proposed to replace $f(x)$ as follow:

$$k(x)=\begin{cases}\gamma x+1 & x<23\eta \\ \eta & x\geq 23\eta\end{cases} \tag{2}$$

in which $\gamma=(\eta-1)/23\eta$

The temperature reduction factor T/T_{max} predicted by Eq. 1 and Eq. 2 are plotted in Figure 5 with respect to the distance x from the fire source. It is worth noting that Eq. 1 can just predict the hot smoke temperature distribution under localised fire. As the flame radiation is taken into account the maximum temperature, T_{max}, will be improved significantly under lower η value [14]. Thus, the simplified model tends to predict more non-uniform temperature distribution with more sharply gradient of η value. But it provides an overall good fit for higher η value as the flame radiation influences on the maximum temperature slightly under less non-uniform temperature distribution.

2.2 Young's Modulus of Cable at Elevated Temperature

Wang et al. [7] experimentally proposed the value of the Young's Modulus of steel cables at elevated temperature and can be fitted by the following equation. Eq. 3 is compared with test data and a good fit is observed as shown in Figure 9.

$$E_T=\frac{E}{0.975+0.007\exp(T/90)} \qquad (20\text{□}\leq T\leq 60\text{□}) \tag{3}$$

where E_T is the Young's Modulus of steel cable at elevated temperature; E is the Young's Modulus of steel cable at ambient temperature (20°C), taken as 1.89×105N/mm^2.

2.3 Stress-strain Relationship of Steel Cable at Elevated Temperature

Wang et al. [7] conducted tests on high tensile steel wires to obtain the mechanical properties at elevated temperature. In this paper, the nonlinear stress strain curves from tests [7] may be approximated using a bi-linear model as shown in Figure 10. The Young's Modulus, E_T, is defined as the slope of linear elastic range. The cable proof stress $f_{y,0.02}^{T}$ is defined as the effective yield strength with proof strain of 0.02, in accordance with EC3 [9]. The yield strength of cables, f_y, is taken as 1690MPa at ambient temperature, and the reduction factor of yield strength for cables at elevated temperature, T, is obtained [7] as:

$$f_{y,0.02}^{T} / f_y = 1.013 - 1.3\times10^{-3}T + 6.179\times10^{-6}T^2 - 2.468\times10^{-8}T^3 + 2.279\times10^{-11}T^4 \quad (4)$$

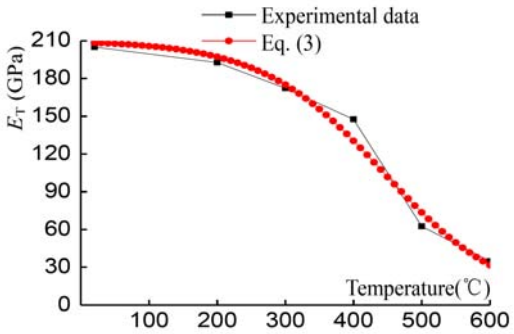

Figure 8. Young's Modulus of Cables at Elevated Temperature - Tests Versus Predicted Formula

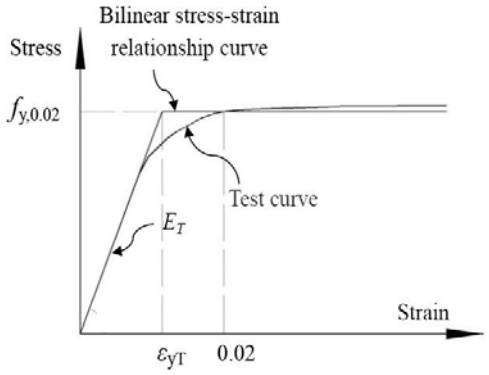

Figure 9. Bi-linear Model to Predict the Stress-strain Relationship of Cable at Elevated Temperature

3. CACULATION OF CABLE TENSILE FORCE UNDER LOCALISED FIRE

When a cable is subjected to a horizontal pre-tensioned force, H_0', its initially curved configuration will change to a straight configuration as shown in Figure 10(a). When the cable is subjected to uniformly distributed load, q_0, along its length, the cable is deformed to a new configuration and cable horizontal tension force changes to H_0, as shown in Figure 10(b). Under a fire situation, the cable will deform further due to the reduction of Young's modulus at elevated temperature. The horizontal tension force in the cable changes to H_{1T} as shown in Figure 10(c).

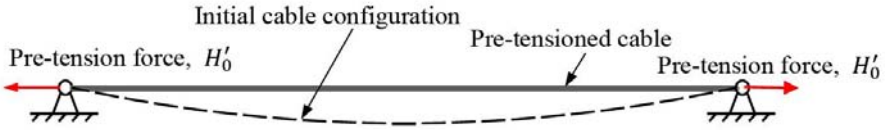

(a) Cable with and without pre−tensioning

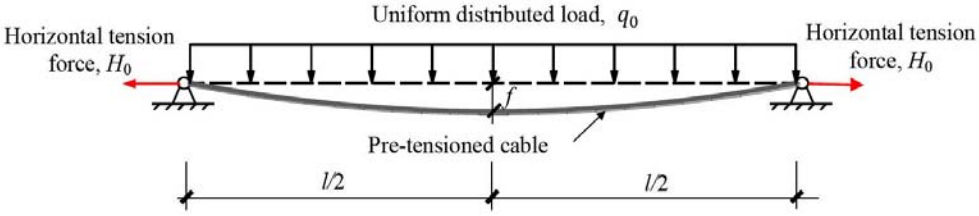

(b) Pre−tensioned cable under uniformly distributed load at ambient temperature

Figure 10. Response of a Pre-tensioned Cable before and during Fire

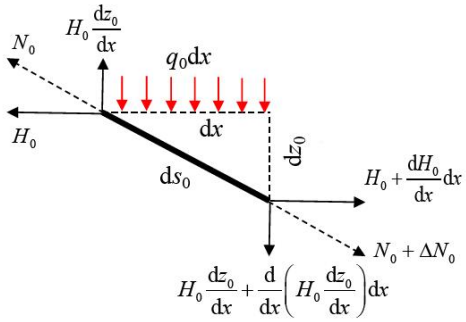

Figure 11. Force Equilibrium of a Differential Element at Ambient Temperature

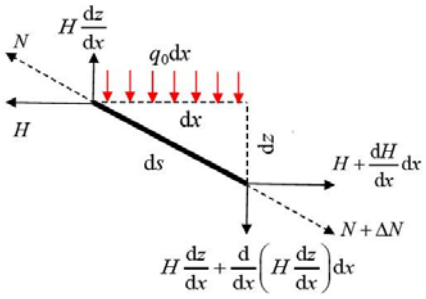

Figure 12. Force Equilibrium of a Differential Element at Elevated Temperature

In order to capture the transient tension force, which is temperature dependent, the force equilibrium equation of a differential cable element can be established at ambient temperature and at elevated temperature as shown in Figure 11 and 12, respectively. The temperature increases from T_0 to T_n given as $\Delta T = T_n - T_0$. If the differential cable element is small enough, the material properties which are temperature dependent will be kept at the same within acable element even though the non-uniform temperature along the length of a cable.

The transient tension force of a cable under uniform distributed load and subject to fire has been derived based on an analytical method proposed in the following sections.

3.1 Cables Subject to Uniform Distributed Loads

A pre-tensioned cable with span, l, and hinged at ends A and B at the same level, is subject to the uniform distributed load, q_0 as shown in Figure 10(b). The cable deflects under a uniformly distributed load, q_0, and the maximum deflection, f, occurs at the mid-span of the cable. The horizontal tension force, H_0, in the cable at ambient temperature can be obtained as reference [2]. At an elevated temperature, the horizontal tensile force changes from H_0 to $H = H_0 + \Delta H$ and the following equation can be obtained based on force equilibrium of a differential element as shown in Figure 13.

$$H\frac{\mathrm{d}^2 z}{\mathrm{d}x^2}+q_0=0 \tag{6}$$

integrating Eq. 6, the following equation can be obtained as:

$$\frac{\mathrm{d}z}{\mathrm{d}x}=\frac{q_0(l-2x)}{2H} \tag{7}$$

as shown in Figure 13, the length of the differential element of a cable can be described as:

$$\mathrm{d}s=\sqrt{\mathrm{d}x^2+\mathrm{d}z^2}=\sqrt{1+\left(\frac{\mathrm{d}z}{\mathrm{d}x}\right)^2}\,\mathrm{d}x \tag{8}$$

similar to Eq. 7, the vertical displacement of the differential element of a cable at ambient temperature as shown in Figure 12 can be written as:

$$\frac{\mathrm{d}z_0}{\mathrm{d}x}=\frac{q_0(l-2x)}{2H_0} \tag{9}$$

thus, the thermal elongation of the differential element for a pre-tensioned cable can be derived as:

$$\mathrm{d}s-\mathrm{d}s_0=\sqrt{1+\left(\frac{\mathrm{d}z}{\mathrm{d}x}\right)^2}\,\mathrm{d}x-\sqrt{1+\left(\frac{\mathrm{d}z_0}{\mathrm{d}x}\right)^2}\,\mathrm{d}x \tag{10}$$

expanding the square root term in Eq. 10 by Taylor series and neglecting the second term, Eq. 10 can be approximated as:

$$\mathrm{d}s-\mathrm{d}s_0=\frac{1}{2}\left[\left(\frac{\mathrm{d}z}{\mathrm{d}x}\right)^2-\left(\frac{\mathrm{d}z_0}{\mathrm{d}x}\right)^2\right]\mathrm{d}x \tag{11}$$

The total thermal elongation of a pre-tensioned cable can then be obtained by integrating Eq. 11 along the length of the cable as

$$\Delta s=\int_l(\mathrm{d}s-\mathrm{d}s_0)\,\mathrm{d}x=\frac{1}{2}\int_l\left[\left(\frac{\mathrm{d}z}{\mathrm{d}x}\right)^2-\left(\frac{\mathrm{d}z_0}{\mathrm{d}x}\right)^2\right]\mathrm{d}x \tag{12}$$

The total strain of a pre-tensioned cable at elevated temperature is the sum of the strain of a cable due to thermal elongation, $\Delta\varepsilon_{\mathrm{th}}$, and that due to the increment of internal tensile force, $\Delta\varepsilon_{\mathrm{N}}$, as:

$$\Delta\varepsilon=\Delta\varepsilon_{\mathrm{th}}+\Delta\varepsilon_{\mathrm{N}}=\alpha\Delta T+\frac{\Delta N}{E_{\mathrm{T}}A} \tag{13}$$

where ΔN is the variation of internal tension force given as $\Delta N=\Delta H\frac{\mathrm{d}s}{\mathrm{d}x}$, α is the coefficient of thermal expansion, and A is the cross section size of a cable.

Integrating Eq. 13 along the cable length, the change of cable length can be obtained as

$$\Delta s=\int_l\left\{\frac{\Delta H}{E_T A}\left[1+\left(\frac{\mathrm{d}z}{\mathrm{d}x}\right)^2\right]\right\}\mathrm{d}x+\int_l\left[\alpha\Delta T\sqrt{1+\left(\frac{\mathrm{d}z}{\mathrm{d}x}\right)^2}\right]\mathrm{d}x \tag{14}$$

Neglecting the higher order term, $\left(\frac{\mathrm{d}z}{\mathrm{d}x}\right)^2$, the above equation can be rewritten as

$$\Delta s=\int_l\frac{\Delta H}{E_T A}\mathrm{d}x+\int_l\alpha\Delta T\,\mathrm{d}x \tag{15}$$

Substituting Δs from Eq. 12 into Eq. 15, and expressing ΔH as

$$\int_l\frac{\Delta H}{E_{\mathrm{T}}A}\mathrm{d}x+\int_l\alpha\Delta T\,\mathrm{d}x=\frac{1}{2}\int_l\left[\left(\frac{\mathrm{d}z}{\mathrm{d}x}\right)^2-\left(\frac{\mathrm{d}z_0}{\mathrm{d}x}\right)^2\right]\mathrm{d}x \tag{16}$$

In the following sections, two fire scenarios will be adopted to analyze the cable: (1) the fire engulfs the entire cable and thus the cable is uniformly heated along its length, and (2) the cable is subject to localized fire and thus the cable is only partially heated at certain portion of the cable length.

Cables subject to Uniform Heating and under uniformly Distributed Load

Substituting Eq. 7 and Eq. 9 into Eq. 16, and integrating the transient horizontal tension force ΔH by assuming uniform heating along the cable length in which the factor of η equals to 1.0 and the cable Young's Modulus remains the same along the length, the cable tensile force can be obtained as:

$$H^2 = \frac{q_0^2 l^2 H_0^2 E_T A}{24H_0^2 H - 24H_0^3 + 24H_0^2 E_T A\alpha\Delta T + q_0^2 l^2 E_T A} \tag{17}$$

The transient horizontal force H in Eq. 17 can be solved by assuming a value of H on the right-hand term and search for the final solution by an iterative process till the right-hand term equal to the left-hand term.

3.2.1 Cables subject to partial heating under uniformly distributed load

When the cable is partially heated under localized fire, the Young's Modulus is varied along the length of cables, depending on it location with respect to fire source. If the area of the fire source is small relative to the length of the cable, the effective radius of fire source, b, in Eq. 1 can be ignored. Substituting Eq. 2 and Eq. 3 into the left side of Eq. 16, we can obtain

$$\int_l \frac{\Delta H\left(975 + 7\exp\left(\frac{T_{\max}k(x)}{90}\right)\right)}{EA\times 10^3}\mathrm{d}x + \int_l \alpha\Delta T k(x)\,\mathrm{d}x = \frac{1}{2}\int_l \left[\left(\frac{\mathrm{d}z}{\mathrm{d}x}\right)^2 - \left(\frac{\mathrm{d}z_0}{\mathrm{d}x}\right)^2\right]\mathrm{d}x \tag{18}$$

The integration zone is shown in Figure 12, while the fire source is right below the cable mid-span, which is dependent on the temperature distribution given by Eq. 2. Since the temperature distribution function is dependent on the length of a cable, the integration zone under centre fire will be classified into two models, that is whether the distance from the vertical axis of plume centre to the end of the cable is over the value of 23η or not. Then, The integration zone of Eq. 18 can be defined as, $0 \le x < \frac{l}{2} - 23\eta$, $\frac{l}{2} - 23\eta \le x \le \frac{l}{2}$, $\frac{l}{2} \le x \le \frac{l}{2} + 23\eta$ and $\frac{l}{2} + 23\eta < x \le l$, as the half length of a cable is not smaller than the value of 23η, shown in Figure 14(a). Otherwise, Eq. 18 will be integrated within the zone, $0 \le x < \frac{l}{2}$ and $\frac{l}{2} \le x < l$, as the half length of a cable is smaller than 23η, as shown in Figure 13(b).

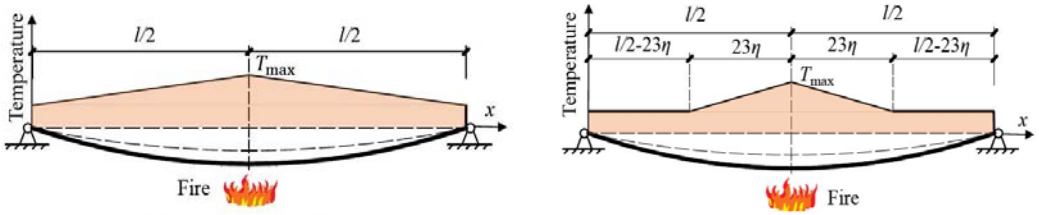

Figure 13. Integration Models along a Cable Dependent of Temperature distribution under Centre Fire

Then, substituting Eq. 7 and Eq. 9 into the right-hand of Eq. 18, the equation of the transient horizontal tension force, which is due to the fire scenario shown in Figure 12, can be obtained as:

$$H^2 = \frac{q_0^2 l^3 H_0^2 EA}{12H_0^2 HB_{nd} - 12H_0^3 B_{nd} + 12H_0^2 EA\alpha\Delta TC_{nd} + q_0^2 l^3 EA} \tag{19}$$

where

if $l/2 \geq 23\eta$, then

$$B_{nd} = \frac{39l}{20} + \frac{63}{25T_{\max}\gamma}\exp\left(\frac{T_{\max}}{90}\right)\left[\exp\left(\frac{T_{\max}\gamma(25-24\eta)}{90}\right)-1\right] + \frac{7}{250}\exp\left(\frac{T_{\max}\eta}{90}\right)\left(\frac{l}{2}-23\eta\right)$$

$$C_{nd} = 2\eta l + 46\eta(1-\eta)$$

if $l/2 < 23\eta$, then

$$B_{nd} = \frac{39l}{20} + \frac{63}{25T_{\max}\gamma}\exp\left(\frac{T_{\max}}{90}\right)\left[\exp\left(\frac{T_{\max}\gamma l}{180}\right)-1\right]$$

$$C_{nd} = 2l + \gamma l^2/2$$

3.3 Pre-tensioned Cables Subject to Point Loads

As shown in Figure 14, a pre-tensioned cable is with the nonlinear geometry shape, s_b, due to gravity load, q_b, at ambient temperature. The horizontal tension force, H_b, can be calculated by Eq. 20.

$$H_b = \frac{q_b l^2}{8f} \tag{20}$$

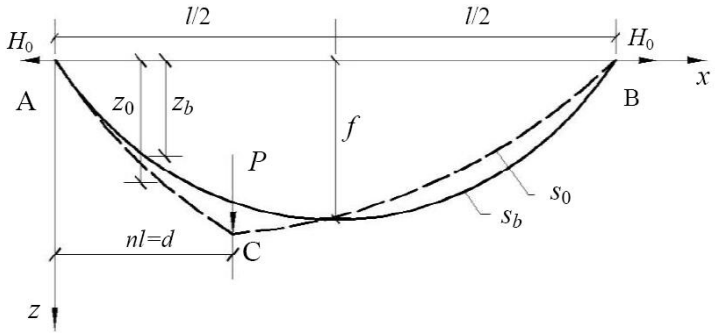

Figure 14. Nonlinear Response of a Pre-tensioned Cable under Point Load at Ambient Temperature

When the cable is subject to a point load, P, at a distance nl from the left support A, the cable geometry changes from the original configuration 's_0' to the deformed geometry 's_b'. The new cable geometry consists of two parabolic segments, AC and CB, with a slope discontinuity at Point C. The following equations can be derived based on the force equilibrium of the cable segments AC and CB [3]

for $0 \leq x \leq d$

$$z_0 = \frac{q_b(l-x) + 2P(1-n)x}{2H_0} \tag{21}$$

for $d < x \leq l$

$$z_0 = \frac{(q_b x + 2Pn)(l-x)}{2H_0} \tag{22}$$

At ambient temperature, Eq. 16 can be rewritten as below

$$\int_l \frac{H_0 - H_b}{EA} dx + = \frac{1}{2}\int_l \left[\left(\frac{dz_0}{dx} \right)^2 - \left(\frac{dz_b}{dx} \right)^2 \right] dx \tag{23}$$

Substituting Eq. 21 and Eq. 22 into Eq. 23, and integrating along the length of a cable, it can be written as:

$$\frac{2(H_0 - H_b)l}{EA} = \frac{12Pq_b d(l-d) + 12P^2 d(1-2n) + 12P^2 n^2 l + q_b^2 l^3}{12H_0^2} - \frac{q_b^2 l^3}{12H_b^2} \tag{24}$$

Let $\xi = 12Pq_b d(l-d) + 12P^2 d(1-2n) + 12P^2 n^2 l + q_b^2 l^3$, the transient horizontal tension force of a pre-tensioned cable under point load at ambient temperature can be derived from Eq. 24 as

$$H_0^2 = \frac{EA\xi H_b^2}{24H_0 H_b^2 l - 24H_b^3 l + q_b^2 l^3 EA} \tag{25}$$

3.3.1 Cables subject to uniform heating along its length under point load

At uniform elevated temperature distribution along the length of the cable, the transient horizontal tensile force in cable increases to $H=H_0+\Delta H$, and induces the nonlinear deformation, z, in a pre-tensioned cable described by as below:

for $0 \le x \le d$

$$z = \frac{q_b(l-x) + 2P(1-n)x}{2H} \tag{26}$$

for $d < x \le l$

$$z = \frac{(q_b x + 2Pn)(l-x)}{2H} \tag{27}$$

Substituting Eq. 21, Eq. 22, Eq. 26 and Eq. 27 into Eq. 16, and integrating along the length of cable, the transient horizontal tensile force of cable under point load with uniform temperature distribution can be obtained as below:

$$H^2 = \frac{H_0^2 D_{ud} E_T A}{8H_0^2 Hl - 8H_0^3 l + 8H_0^2 E_T A\alpha\Delta Tl + D_{ud} E_T A} \tag{28}$$

with $D_{ud} = q_b^2 l^3 / 3 + 4Pq_b d(l-d) + 4P^2(1-2n)d + 4P^2 n^2 l$

3.3.2 Cables subject to non-uniform heating along its length under point load

The regions for integrating Eq. 16 is taken as $0 \le x < l/2 - 23\eta$, $l/2 - 23\eta < x < nl$, $nl < x < l/2$, $nl < x < l/2 + 23\eta$ and $l/2 + 23\eta < x < l$ if the half length of cable is greater than the value of 23η, as shown in Figure 15(a). Otherwise, Eq. 16 shall be integrated within the zone of $0 \le x < l/2$ and $l/2 \le x < l$ as the half length of cable is smaller than 23η, as shown in Figure 15(b). The horizontal tensile force in the cable under point load exposed to non-uniform heating distribution can be obtained as:

$$H^2 = \frac{H_0^2 D_{ud} E_{20} A}{4H_0^2 HB_{nd} - 4H_0^3 B_{nd} + 4H_0^2 E_{20} A\alpha\Delta TC_{nd} + D_{ud} E_{20} A} \tag{29}$$

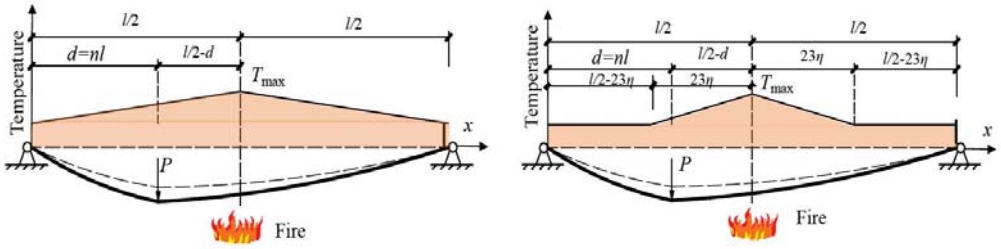

Figure 15. Integration Model along a Cable dependent of Non-uniform Temperature distribution under Centre Fire with Point Load, P

4 CASE STUDY

As shown in Figure 10(b), the cable is subject to a pre-tensile force of H_0=19.1 kN and under the uniformly distributed load of q_0=0.5 kN/m. The length of the cable is 8m, and the cable cross sectional area is 0.674 cm^2. Young's Modulus, E, at ambient temperature is 1.89×105 MPa. Assuming the cable is fully engulfed in fire and it is subjected to uniform heating along its entire length, the transient horizontal tension force in the exposed to uniform heating can be obtained as follow.

Assuming a temperature of 250℃, the Young's Modulus of the cable can be calculated from Eq. 3 as $E_T = 1.78\times10^5 \text{MPa}$. Substituting the values of H_0, A, l, q_0, E_T, into Eq. 17 and obtain:

$$H^2 = \frac{7975}{H + 44.6} \tag{30}$$

The transient horizontal tension force, H, from Eq. 30 can be calculated using an iterative method and a final value of H = 11.9kN is obtained. A similar method is then repeated to calculate H for cable subject to another temperature and the relationship between H and temperature, T, is plotted as shown in Figure 16.

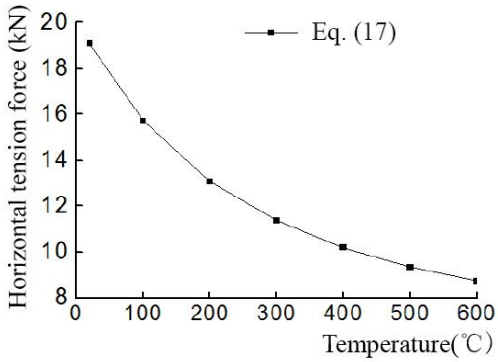

Figure16. Horizontal Tension Force against Temperature

For other loading configuration and temperature distributions, the transient horizontal tension force in the cable can be obtained from Eq. 19, Eq. 28 or Eq. 29, respectively.

5. LOAD RESISTANCE OF PRE-TENSIONED STEEL CABLES UNDER FIRE

The transient horizontal tension force of pre-tensioned cables under uniform distributed load or point load exposed to local fire scenarios can be calculated by the proposed equations while the effective yield strength of cables dependent on the elevated temperature can be obtained from Eq. 4. The fire resistance or critical temperature of a pre-tensioned cable can be determined when the tension force is equal to the yield load of the cable. The following example illustrates the procedure of calculating the fire resistance of pre-tensioned cable subjected to localized fire.

At fire limit state, the load resistance of a pre-tensioned cable is dependent on the maximum temperature according to Eq. 1 and temperature distribution as shown in Figure 5. For long span cable, if the vertical displacement of a cable is small enough, the tension force in cables will be similar to the horizontal tensile force. Then, the stress of a pre-tensioned cable should be satisfied by the equation as:

$$\sigma_{\mathrm{T}}=\frac{H}{A}\leq f_{y,0.02}^{T} \tag{31}$$

where σ_{T} is the stress of a pre-tensioned cable at elevated temperature; A is the size of cross section of a cable; H is the transient horizontal tensile force at elevated temperature, obtained by Eq. 17, Eq. 19, Eq.28 or Eq. 29 respectively; $f_{y,0.02}^{T}$ is the yield strength of a cable dependent on temperature, obtained by Eq. 4.

For example, a pre-tensioned cable with the size of cross section, A=0.674 cm^2; and Young's Modulus as E =1.89×105MPa. The span length of the cable is l = 20m; horizontal tension force at ambient temperature is H_{b} = 11.53kN; uniformly distributed dead load is q_0=0.2 kN/m; point force P =1kN is acting at 0.5l from the support. The temperature reduction factor is taken as η=0.6 .A numerical model of pre-tensioned cable mentioned above has been established by using ANSYS software shown in Figure 17. The 'Link8' element has been employed to simulate the pre-tensioned cable. As Shown in Figure 18, the numerical model of pre-tensioned cable designed as above is modelled by the Link 8 elements and cut into one hundred elements along its length. The horizontal tension force and the tensile stress in the cables computed by the numerical analyses and from Eq. 29 are compared as shown in Figure. 20 and 21, respectively.

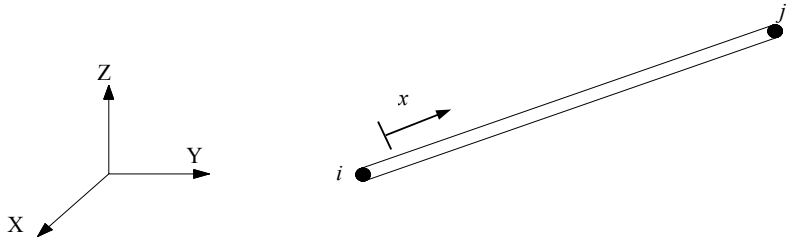

Figure 17. Numerical Model of Link 8 Element

Figure 18. Numerical Model of a Pre-tensioned Cable

According to the Eq. 1, the temperature distribution along the pre-tensioned cable can be updated by tracing the maximum temperature, T_{max}, with 10℃ interval. Under each temperature distribution, the tension force, H, can be calculated by Eq. 17, Eq. 19, Eq. 28 or Eq. 29, and then, checked by Eq. 31 step by step.

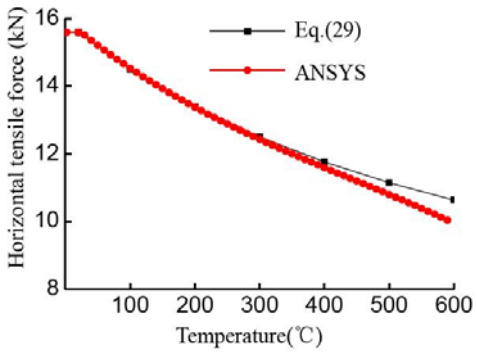

Figure 19. Horizontal Tension Force of the Pre-tensioned Cable at Elevated Temperature

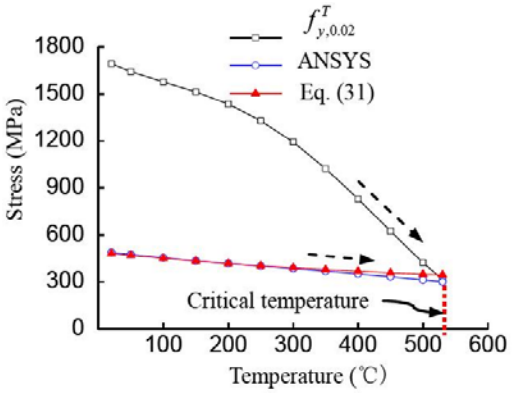

Figure 20. Mechanical Response of the Pre-tensioned Cable at Elevated Temperature

Figure 16 shows that the horizontal tension force calculated from Eq. 29 decreases with the temperature rise and fits the numerical result well in lower temperature range. Above 400℃, there is somewhat a difference between Eq. 29 and numerical results. The maximum amount of deviation reaches 7% at 600℃ because the higher order term, $(dz/dx)^2$, is ignored in Eq. 14.

The yield strength of the steel cable at elevated temperature is also plotted in Figure 20. When the tensile stress of the steel cable meets the yield strength, the fire resistance temperature or critical temperature is attained. Figure 20 also shows that the tensile stress in the cable obtained from the numerical simulation and a good fit with the analytical result is observed. It indicates that the equations of the transient horizontal force developed in the present studies can provide a good estimate of the mechanical response of pre-tensioned steel cable subjected to localized fire.

The following section investigates the key parameters that influence the mechanical behavior of pre-tensioned cables under localized fire.

6. FACTORS AFFECTING THE CABLE TENSILE FORCE UNDER FIRES

Tension force in cables represents the key mechanical characterizes of pre-tensioned cables. The initial tension force level, load ratio, span of cables and the degree of non-uniform temperature distribution along the length of the cable are involved in Eq. 17, Eq. 19, Eq. 28 and Eq. 29, which determines the transient tension force in cables.

Firstly, the pre-tension level, P_r, is defined as the pre-tension force, H_0', forming the nonlinear geometric shape before loading, shown in Figure 9(a), to yield strength at ambient temperature as:

$$P_r = \frac{H_0'}{f_y A} \tag{32}$$

In Eq. 32, the pre-tension force is always designed as lower than 30% yield strength at ambient temperature [2].

Load ratio, R, is the horizontal tension force of cables due to load, shown in Figure 10(b), to yield strength at ambient temperature as below.

$$R = \frac{H_0}{f_y A} \tag{33}$$

6.1 Effects of Pre-tensioned Force Level

To study the effects of pre-tensioned force level on the horizontal tension force of cables at elevated temperature, an example has been designed as below.

The pre-tensioned steel cable under uniform distributed load, shown in Figure 10(c), with the cross section of 0.674 cm^2;Young's Modulus of 1.89 × 105 MPa; cable span of 20m; load level of 0.4;the non-uniform temperature distribution with the reduction factor, $\eta = 0.6$;the initial pre-tension force level, P_r , ranged of 0.1 to 0.18.

At ambient temperature, the initial geometrical configuration of a cable is significantly dependent on the pre-tension force before loading. The cable will be stretched more tightly and induced the less displacement at the mid-span with higher pre-tension force level.

As shown in Figure 10(a) and 10(b), the horizontal tension force, H_0' , can be updated to H_0, due to uniform distribution load, that is, the horizontal tension force, H_0, is affected by pre-tension force, H_0' , and uniform distribution load, q_0. In order for parametric analysis to keep the given load level, R=0.4, constant, the horizontal tension force, H_0, should be kept constant according to the Eq. 33. Meanwhile, the pre-tension force level increases as listed in table 2 to analyze its effect on the mechanical behaviors of pre-tensioned cables under localized fire. According to the Eq. 32, the pre-tension force, H_0' , increases while the pre-tension force level increasing. Thus, the uniform distribution load, q_0, should be decreased while the pre-tension force increases to keep the horizontal tension force constant.

Table 2. Pre-tension Force Level under the Uniform Distribution Load

Pre-tension force level, P_r	0.10	0.12	0.14	0.16	0.18
Uniform distribution load, q_0 (kN/m)	2.130	1.788	1.540	1.355	1.215

Resulting from the Eq. 19, at each elevated temperature level, the horizontal tension force of the cable decreases with the increase of the pre-tensioned force level at each temperature level, as shown in Figure 21. When comparing with the horizontal tension forces in the cable which resulted from numerical analysis and Eq. 19 at elevated temperature, it is discovered that they hold the same tendency, that is, with the tension force level increasing, the horizontal tension force decreases more sharply under localized fire.

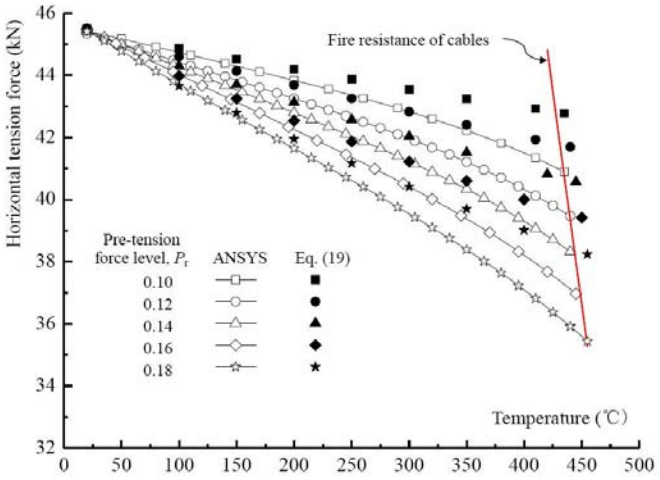

Figure 21. Horizontal Tension Force vs. Temperature in a Range of Pre-tensioned Force Level

As shown in Figure 21, the maximum deviation of the horizontal tensile force is 7.3% between the curves resulted from Eq. 19 and numerical simulation using by ANSYS software. It proves that the numerical analysis can simulate the mechanical behaviors of cables under localized fires enough. It should be noted that the critical temperature of the pre-tensioned steel cable is dependent on the pre-tension force level, temperature distribution and the fire resistance of cables together under the same load ratio. Hence, according to the same failure state which is shown in Figure 21, when the curve of horizontal tension force drops more sharply, it meets the fire resistance curve, which decreases through the whole temperature history, more lately and led to the higher critical temperature as the pre-tensioned force level increasing.

6.2 Effects of Load Ratio

In order to study the effects of load ratio on the horizontal tensile force of cables at elevated temperature, the cable with the same geometric properties given in the 5.1 section of this paper is with the pre-tensioned force level, $P_r = 0.1$; the reduction factor of the temperature distribution is taken as $\eta = 0.6$;the load ratio, R, in a range of 0.2 to 0.7.

A range of horizontal tension force at ambient temperature, H_0, can be obtained by Eq. 33 under each load ratio. It should be noted that the horizontal tension force, H_0, increases with the increasing of the load ratio at ambient temperature. In order to keep the increasing of the horizontal tension force, the uniform distribution load should be increased as listed in table 3.

Table 3. Load Ratio under the Uniform Distribution Load

Load ratio, R	0.2	0.3	0.4	0.5	0.6	0.7
Uniform distribution load, q_0 (kN/m)	1.03	1.575	2.13	2.71	3.28	3.88

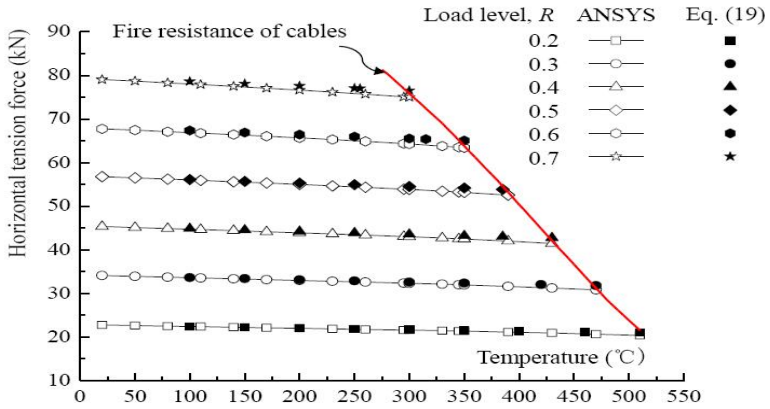

Figure 22. Horizontal Tension Force Versus Temperature History in a Range of Load Ratio

Resulting from the Eq. 19, at each elevated temperature level, the horizontal tension force in the cable is increasing dramatically with the increasing of load ratio at each temperature level, shown in Figure 22. Comparing with the horizontal tension forces in the cable resulted from numerical analysis and Eq. 19 at elevated temperature, they fit well together with 3.2% deviation between the curves resulted from Eq. 19 and numerical simulation using by ANSYS software, and the horizontal tension force is decreasing slightly at the same gradient through the whole temperature history.

Checking with Eq. 31, the curve of the horizontal tension force met the fire resistance curve earlier and led to the lower critical temperature as the load ratio increasing.

6.3 Effects of Non-uniform Heating Along the Length of Cables

In order to study the effects of the non-uniform temperature distribution on the horizontal tension force in cables at elevated temperature, the cable with the same geometric properties given in the 5.1 section of this paper is with the pre-tension force level, $P_r = 0.1$; the load ratio, $R = 0.3$; uniform distribution load, $q_0 = 1.575\text{kN/m}$; and the non-uniform heating along the length of the cable with the reduction factors in a range of, η=0.2~1.0.

Resulting from the Eq. 19, at each elevated temperature level, the horizontal tension force in the cable is decreased with the increasing of temperature reduction factor, shown in Figure 23. The comparison with the horizontal tension forces in the cable resulted from numerical analysis and Eq. 19 at elevated temperature, the maximum deviation of the horizontal tension force is 5.3%.

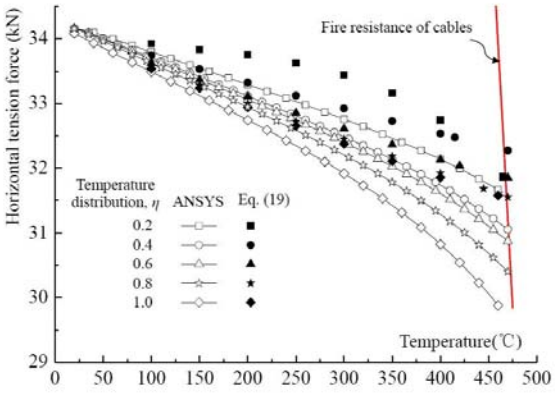

Figure 23. Horizontal Tension Force Versus Temperature History in a Range of Temperature Distribution

The horizontal tension force is decreasing more sharply with the larger temperature reduction factor, that is, the more uniform temperature distribution can lead to the horizontal tension force dropping more sharply and meeting the fire resistance curve more lately. Checking with Eq. 31, the curve of the horizontal tension force met the fire resistance curve more early with the more non-uniform temperature distribution and led to the lower critical temperature. As the uniform temperature distribution with $\eta = 1.0$, the element at the end of a cable may fall to failure much earlier than that with a little lower tension force at the mid-span of a cable.

6.4 Effects of the Cable Span Length

As shown in Figure 24, a longer cable will be exposed to the more concentrate heated zone along its length. Therefore, the cable length should be one of the key factors which would influence the horizontal tension force in cables at elevated temperature.

In order to study effects of the cable span length on the horizontal tension force in a cable at elevated temperature, the cable with the same geometric properties given in the 5.1 section of this paper is with the pre-tension force level, $P_r = 0.1$; the load ratio, $R = 0.5$; the non-uniform heating along the length of the cable with the reduction factors, $\eta = 0.6$, and the span length of the cable in a range of 12m ~ 32m.

In order to keep the constant value of the horizontal tension force, H_0, the load, q_0, should be updated with the length of the cable increasing as listed in table 4.

Table 4. Pre-tension Force Level against the Uniform Distribution Load

Length of the cable, l (m)	12	16	20	24	28	32
Uniform distribution load, q_0 (kN/m)	2.87	2.75	2.705	2.69	2.71	2.73

Resulting from the Eq. 19, at each elevated temperature level, the horizontal tension force in the cable decreases with a decrease of the length of cables at each temperature level, as shown in Figure 24. Comparing with the horizontal tension forces in the cable resulted from numerical analysis and Eq. 19 at elevated temperature, the maximum deviation of the horizontal tension force is 6.6%.

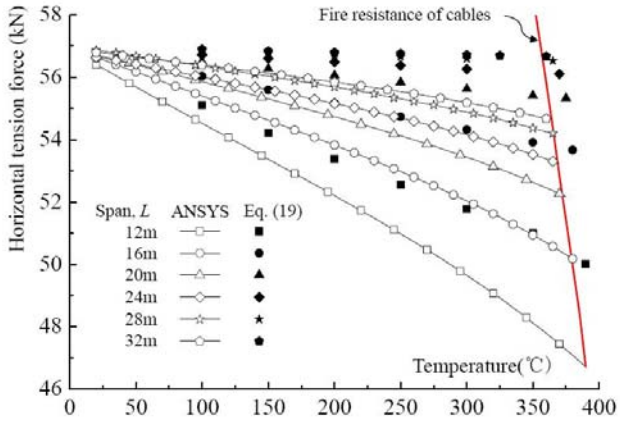

Figure 24. Horizontal Tension Force under Temperature History in a Range of Span

The horizontal tension force decreases more sharply with the shorter span of cables, that is, the localized fire will influence the horizontal tension force in the shorter span cables more greatly. Checking with Eq. 31, the curve of the horizontal tension force met the fire resistance curve more early with the larger span and led to the lower critical temperature.

6.5 Effects of the Moving Fire

Movement of fire is one of the typical features of localized fires in nature. As shown in Figure 25, as the fire moves away from the center, the non-uniform temperature distribution with factor, η=0.6, is no longer symmetrical to the mid-span of cables. When the fire moved from point A to point B, as shown in the insert of Figure 25, the tension force distribution along the length of a cable kept symmetrical to the mid-span of cables, and the value of the tension force increased slightly. It should be worth noting that the tension force at the mid-span of the cable decreases only by about 10% from that at the end of cable. The gradient of tension force along the large span of cable is rather low. It can be assumed that the tension force is almost uniform distribution along the cable. On the other hand, the fire resistance of cable decreases significantly as temperature increases, as shown in Figure 20. Thus, the centre fire scenario is considered to be more critical and can be used to evaluate the fire safety of a pre-tensioned cable.

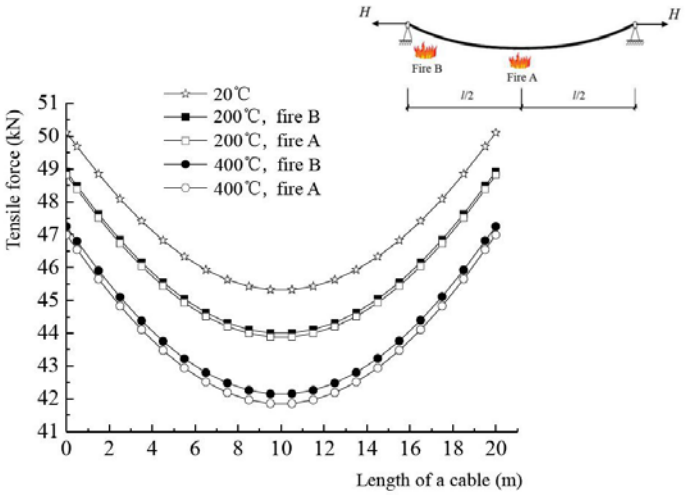

Figure 25. Tension Force Distribution along the Length of a Cable under Moving Fire

7. DESIGN OF PRE-TENSIONED CABLES FOR FIRE SAFETY

Figure 26 outlines a design flow chart without using sophisticated numerical software to determine the fire safety of a pre-tensioned cable subject to localised fire. The ability of a pre-tensioned cable to sustain the applied load under localised fires is considered the yield strength and Young's modulus of cables dependent on the non-uniform temperature distribution along the length of the cable. Two design strategies have been proposed to improve the fire resistance for pre-tensioned cables based on the influence parameters analysis illustrated above and thermal transfer respectively.

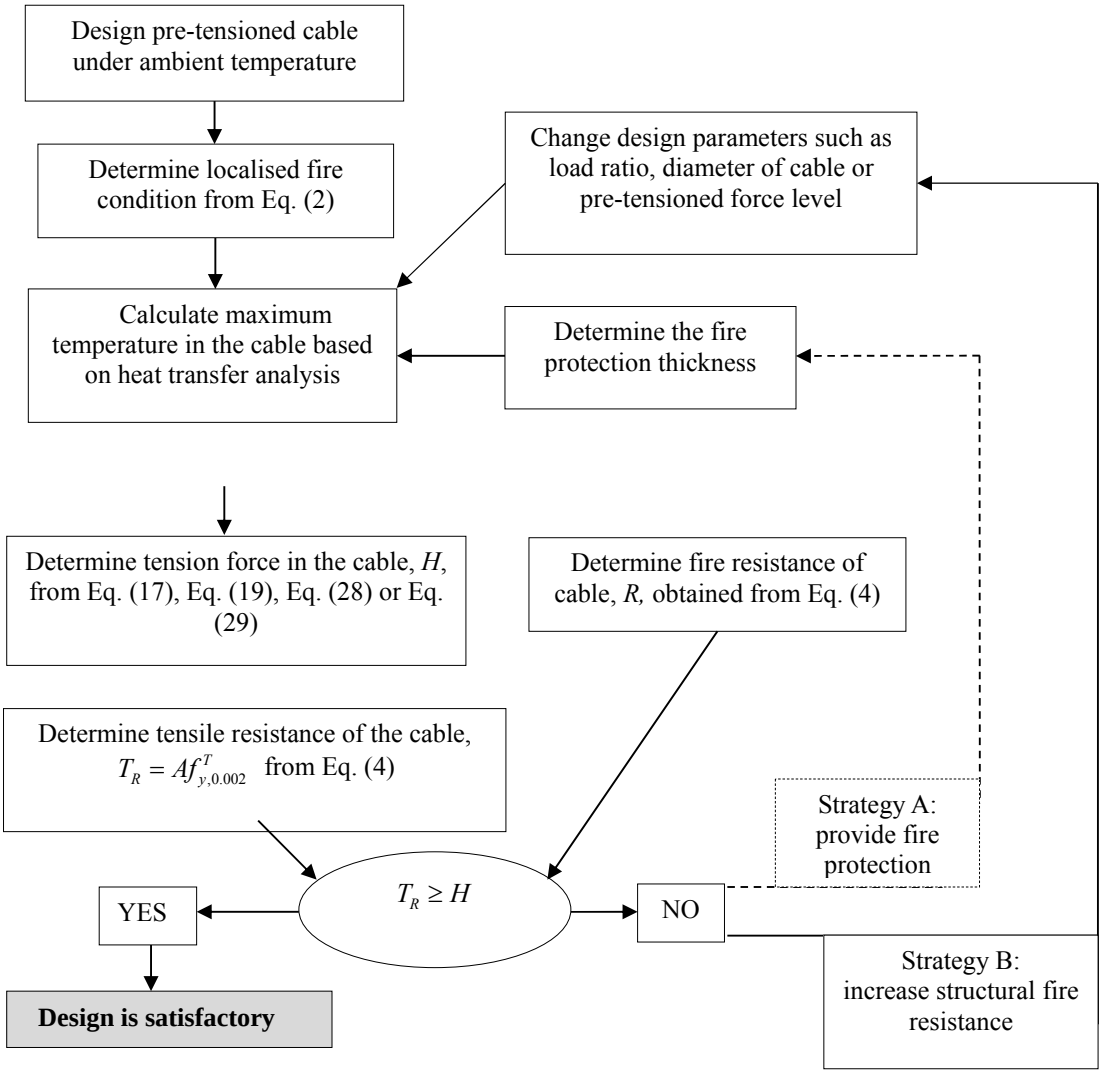

Figure 26. Design Flow Chart for Pre-tensioned Cables at Localised Fire

7. CONCLUSIONS

In this study, an analytical method has been proposed to determine the mechanical behaviour of pre-tensioned steel cables subjected to localised fire. The horizontal tensile force subjected to localised fire is influenced by the load ratio, pre-tensile force level, length of cables, temperature distribution along the cable length and material properties at elevated temperature. Analytical methods have been developed to predict the horizontal tensile force in cable under different fire scenarios which consider uniform or non-uniform heating along the cable length with point load or uniform distributed load.

The critical temperature of the cable can be determined when the horizontal tensile stress reaches the effective yield strength of the cable at elevated temperature. The accuracy of the proposed analytical method is verified against the results obtained by nonlinear finite element analysis. Parametric studies have been conducted and the results show that:

- The horizontal tension force in cables decreased more sharply as the pre-tensioned force level increases.
- The horizontal tensile force in cables increases with the increase of load ratio and decreases with the increase in temperature.
- The horizontal tension force decreases more sharply with the degree of the non-uniform temperature distribution along the length of a cable.
- The horizontal tensile force decreases more sharply with the shorter span of cables in the same temperature distribution in localised fire.
- The horizontal tension force in cables is not affected significantly by the location of the fire. The critical location of the fire source is identified to be the one located just below the mid-length of the cable.

Finally, the design flow chart for pre-tensioned cables at localized fire has been proposed to estimate the fire safety of cables. The results from parametric analyses are useful to formulate design guide to evaluate the fire safety of pre-tensioned structures.

ACKNOWLEDGE

The authors gratefully acknowledge the financial support of the Civil Engineering Disaster Prevention National Key Laboratory in China, and the International Structural Fire Research Laboratory (ISFRL) in Nanjing Tech University, China.

REFERENCES

[1] Saitoh, M. and Okada, A., “The Role of String in Hybrid String Structure”, Engineering Structures, 1999, Vol.21, pp.756–769.
[2] Shen, S.Z., Xu, C.B. and Zhao, C., “Design of Cable Structures”, China Architecture & Technology Press”, 2006. (in Chinese)
[3] Krishna, P. “Cable Suspension Roofs”, Kingsport Press, USA, 1978.
[4] Zhou, H.T., “Study on Fire Resistance Performance of Saddle Cable Net Structures”, Ph.D thesis, Tongji University, Shanghai, China, 2006. (in Chinese)
[5] Sheng, H.M., “Research on Mechanics Behaviors with Analytical Solutions and Numerical Simulation for Beam String Structures under Localized Fire”, Ms.D thesis, Nanjing Tech University, Nanjing, China, 2014. (in Chinese)

[6] Fan, D.H., "Research on Failure Modes of Kiewitt-Lamella Suspension Domes under Localized Fire", Ms.D thesis, Nanjing Tech University, Nanjing, China, 2015. (in Chinese)
[7] Wang, Y., Shen, Z. and Li, Y., "Experimental Study of the Mechanical Properties of Pre-stressed Steel Wire at Elevated Temperatures", International Conference on Structures in Fire, USA, 2010.
[8] Society of American Post-tensioned Concrete, East China Technology Development Center of Pre-stressed Concrete. Pre-tensioned Concrete Manual. Southeast University Press, Nanjing, 1989.
[9] EN 1991-1-2 (1992), Eurocode 1–Actions on Structures. Part 1-2. General Actions – Actions on structures exposed to fire. European Committee for Standardization, Brussels, 2013.
[10] ASTM (2005), Standard methods of fire tests of building construction and materials, ASTM Standard E119-05, American Society for Testing and Materials, West Conshohocken, PA.
[11] NFPA (2006), Standard methods of tests of fire Endurance of Building Construction and Materials. NFPA 251. National Fire Protection Association, Quincy, MA.
[12] National Institute of Standards for Engineering. Technical Code for Fire Safety of Steel Structures in Buildings. CECS 200：2006, China.
[13] Du, Y. and Li, G.Q., "A New Temperature Curve for Analysis of Structural Fire-resistance", Fire Safety Journal, 2012, Vol. 54, No. 11, pp.113-120.
[14] Du, Y. and Li, G.Q., "Effects of Flame Radiation on Temperature Elevation of Steel Members in Large Space Building Fire", International Conference on Application of Structure Fire Engineering, Prague, Czech Republic, 2009, pp.356-361.